Title: Spatio-temporal patterns of genetic diversity in the Mediterranean striped dolphin (*Stenella coeruleoalba*)

Running title: Dolphin spatio-temporal genetics

Stefania Gaspari[1], *Letizia Marsili*[2], *Chiara Natali*[3], *Sabina Airoldi*[4], *Caterina Lanfredi*[4], *Charles Deeming*[5], *André E. Moura*[5]

[1]*CNR – Istituto di Scienze Marine, Ancona, Italy*
[2]*Department of Environmental Science, University of Siena, Siena, Italy*
[3]*Department of Biology, University of Florence, Florence, Italy*
[4]*Tethys Research Institute, Milan, Italy*
[5]*School of Life Sciences, University of Lincoln, Lincoln, UK*

Corresponding author*:* Andre E. Moura, amoura@lincoln.ac.uk, Tel: +44 (0)1522886805

Keywords: microsatellite loci, control region, morbillivirus, environmental stress, genetic variability, Mediterranean Sea

ABSTRACT

Comparing the genetic composition of wild animals between geographic regions with distinct environments is common in evolutionary studies. However, genetic composition can also change through time in response to environmental changes but studies examining this are carried out less often. In this study, we characterise striped dolphin genetic composition in the Mediterranean Sea across both geography and time. We provide genotype data for 15 microsatellite loci and 919 bp of mtDNA control region, collected over 21 years across all main Mediterranean Sea basins.

We investigated spatial genetic structure using both classical and Bayesian population structure methods, and compared it with temporal patterns of genetic change using time series statistics. We integrated the temporal datasets with known environmental pressures and data on social structure, to infer potential drivers of observed changes.

Geographic analyses suggest weak differentiation for striped dolphin in the Mediterranean Sea, with evidence for a recent expansion. Temporal analyses show significant cyclical fluctuations in genetic composition over 21 years, which correspond well with recurrent morbillivirus epizootics. Similarly, social group composition shows changes in the relative number of juveniles and adults per group, and an overall increase in the number of adults per group relative to juveniles over the time period. We suggest that the observed changes in genetic and group composition could relate to specific dynamics of morbillivirus resistance. Overall, our study highlights the importance of tracking long term genetic variation, and the potential for this species as a model in studying genetic adaptation to environmental stress.

INTRODUCTION

Genetic diversity of wild animals can be influenced by several factors, namely phylogeographic patterns, demographic fluctuations caused by external pressures, and patterns of social behaviour. Although studies of genetic variation in a geographic context have been common, studies tracking changes in genetic variation over time are more difficult to achieve. Previous examples have focused on animals with a restricted geographic distribution (e.g. Clutton-Brock & Pemberton, 2004), or species of small size whose identification and capture are relatively simple (e.g. Pilot, Dąbrowski, Jancewicz, Schtickzelle & Gliwicz, 2010; Turner et al., 2014). For large animals distributed over wide geographic ranges, logistic difficulties make studying genetic variation over both space and time particularly challenging.

However, analyzing genetic variation through time can also provide useful insight, as extreme demographic events can change allele frequencies and dilute genetic signals of more subtle events (e.g. Moura, Natoli, Rogan & Hoelzel, 2013), while reduced genetic diversity can increase quickly in wild populations following demographic bottlenecks (Lovatt & Hoelzel, 2013). Genetic information can then be correlated with known environmental pressures, to gain a better understanding of the factors driving genetic variation and structure. In this study, we analysed patterns of genetic variation in both space and time for the Mediterranean population of striped dolphin (*Stenella coeruleoalba*, Meyen 1833), and correlated the observed changes with known environmental pressures and changes in group composition.

The striped dolphin is the most common cetacean in the Mediterranean Sea (Gaspari, Azzelino, Airoldi & Hoelzel, 2007). Previous studies suggest that striped dolphins in the Mediterranean basin are genetically differentiated from the Atlantic Ocean (Garcia-Martinez, Moya, Raga & Latorre, 1999; Bourret, Macé & Crouau-Roy, 2007; Gaspari et al., 2007), with further subdivision within the Mediterranean Sea being suggested by kinship analysis (Gaspari et al., 2007) and factorial analyses (Gkafas et al., 2017). Furthermore, in the last three decades the striped dolphin has faced ecological pressure from a series of morbillivirus epizootics across the Mediterranean basin (Di Guardo & Mazzariol, 2013). The earliest during 1990-1992 was particularly severe, with thousands of animals succumbing to the disease (Cebrian, 1995). Since then, other epizootic episodes have been described, and although the strength of supporting evidence varies, a 3-5 years cycle of occurrence has been suggested (Di Guardo & Mazzariol, 2013). Cetacean morbillivirus (CeMV) was first recognized formally about 20 years ago, and is considered one of the most pathogenic virus in cetaceans (Barrett et

al., 1993; Lipscomb et al., 1996; Taubenberger et al., 2000; Van Bressem et al., 2014), with large die-offs described worldwide (Van Bressem et al., 2014).

Therefore, a temporal description of genetic variation as this dolphin species experienced various epizootics, is an important first step into understanding the effects morbillivirus can have on the genetic composition of this population. In this study, we look at genetic variation in 15 microsatellites and mitochondrial DNA control region (CR) for a nearly complete time-series of samples obtained between 1998 and 2008, during which striped dolphins experienced several morbillivirus epizootics. Although other cetacean species in the Mediterranean Sea were affected (e.g. Di Guardo et al., 2013), striped dolphins appear particularly susceptible to morbillivirus epizootics. The reasons for this are still unclear, with suggestions of both intrinsic factors (e.g. large group sizes) and extrinsic factors (e.g. environmental contamination; Aguilar & Borrell, 2005) playing important roles. Low genetic diversity from high inbreeding has also been suggested as a main cause of the increased susceptibility (Valsecchi, Amos, Raga, Podesta & Sherwin, 2004). However, reduced genetic diversity might also result from a recent expansion into the Mediterranean basin, as shown for the bottlenose dolphin (Gaspari et al., 2015). Our understanding of the role that reduced genetic variation (e.g. inbreeding) can have on pathogen susceptibility, can be improved by tracking genetic variation levels during the course of repeated epizootic events.

Objectives

In this study, we analyse the most comprehensive dataset of genetic data for striped dolphins in the Mediterranean Sea to date. Our dataset includes representatives of all the main Mediterranean oceanographic basins, and represents 22 years of genetic monitoring (1987 to 2009) during which the species experienced multiple epizootics with large levels of mortality (Van Bressem et al., 2014). All samples were genotyped for 15 microsatellite loci and for CR, thus providing a multilocus individual based analysis of population structure and phylogeography. Furthermore, we compared genetic data with social group composition data (e.g. age categories), to evaluate the potential for changes in social structure during the time period. This study represents a remarkably long term high resolution analysis of genetic variation changes in a wild dolphin population, in response to a well described external ecological pressure. It not only contributes to our understanding of the relationship between genetic diversity and ecological factors, but also to the conservation of local wildlife. Due to their abundance and wide distribution, striped dolphins could act as a reservoir of morbillivirus, which could then spread to other Mediterranean mammals, some of which are

111 critically endangered.
112
113 **MATERIALS AND METHODS**
114 **Sample collection and genotyping**
115 Tissue samples from 368 adult striped dolphins were collected between 1987 and 2009
116 from stranded (s) and free-ranging (fr) specimens across the Mediterranean Sea (Figure 1 &
117 Table S1). Although we did not determine whether the sampled animals were infected with
118 morbillivirus, during epizootics a stranded animal had a higher probability of being infected.
119 Therefore, the use of both stranded and biopsy samples, considerably minimises the potential
120 bias from representation of diseased or resistant animals during the epizootics. All samples
121 were genotyped for microsatellite loci, with 131 being genotyped for mitochondrial DNA
122 control region (CR), with 111 genotyped for both microsatellites and CR.
123 DNA was extracted using a standard phenol/chloroform and ethanol precipitation
124 protocol, from tissue samples preserved in salt saturated 20% DMSO solution. Nuclear DNA
125 was genotyped for 15 microsatellite loci, including KWM1b, KWM2a, KWM2b, KWM12a
126 KWM5c, EV37Mn, D08, Sco11, Sco65, Sco66, Dde59, Dde61, Dde66, Dde70, Dde72 (see
127 Bourret, Macé, Bonhomme & Crouau-Roy et al. 2008 for original sources). Amplification
128 was carried out through five multiplex PCRs, in a total volume of 10 µl with 50 ng of total
129 DNA, 1×PCR buffer, 1.5 mM $MgCl_2$, 300 µM of each dNTP, 0.5 µM of each primer, and 0.5
130 units of Taq DNA polymerase. Thermal profiles consisted of an initial denaturation step of 5
131 min at 94 °C, followed by 35 cycles of 45 s at 94 °C, 45 s at the respective annealing
132 temperature, and 30 s at 72 °C, with a final extension step of 10 min at 72 °C. Details of the
133 annealing temperatures and composition of each multiplex are provided in the supplementary
134 Table S2. Amplicons were resolved by capillary electrophoresis in an Applied Biosystems
135 3100xl Genetic Analyzer and allele sizes scored against a GeneScan500 ROX size standard
136 using GeneMapper 5.0 (Applied Biosystems).
137 To ensure accuracy of genotypes, each sample was amplified and genotyped at least twice,
138 with 60% of samples being processed 3 times. Three different researchers scored all samples
139 independently. Genotypes were screened for duplicates using MStools 3.1, with 4 samples
140 being removed after screening, reducing the total to 364. The dataset was checked for
141 genotyping or scoring errors due to null alleles using Microchecker v. 2.2.3 (van Oosterhout,
142 Hutchinson, Wills & Shipley, 2004). Original genotypes are available in the Mendeley dataset
143 with DOI 10.17632/47sr5sgjhm.1. .
144 The mitochondrial control region (CR) was amplified using oligonucleotide primers

designed for the genes at both the 5'and 3'ends of the CR (tRNA Thr and 12S genes; Gaspari et al., 2015). Predicted amplification size using this primers is 1 265 bp, with final alignment having a length of 919 bp. PCR was conducted in a total volume of 15 µl with 100 ng of total DNA, 1×PCR buffer, 1.5 mM $MgCl_2$, 200 µM of each dNTP, 0.5 µM of each primer, and 0.5 units of Taq DNA polymerase. The PCR cycling profile was 4 min at 95 °C, 35 cycles of 45 s at 94 °C, 1.5 min at 50 °C and 1.5 min at 72 °C followed by 8 min at 72 °C. Amplicons were diluted in DNA-ase and RNA-ase free water and they were cycle-sequenced using BigDye Terminator V3.1 chemistry according to the manufacturer's protocol (Applied Biosystems). The products were cleaned with isopropanol and resolved on an Applied Biosystems 3100 xl Genetic Analyzer. Sequencing was done in forward and reverse directions on an ABI 3100 sequencer, and only genotypes that matched between the two reactions were considered valid. All sequences were aligned using CodonCode Aligner Software (CodoneCode Corporation). Alignment of all sequences is available in the Mendeley dataset with DOI 10.17632/47sr5sgjhm.1.

Comparing CR sequences produced in this study with previously published sequences worldwide

All CR sequences produced in this study were aligned with the CR region of other cetacean species, obtained from mitogenomic sequences in (Moura et al. 2013) and extracted from the NCBI nucleotide database. A Neighbour-Joining tree was then constructed, using the Jukes-Cantor genetic distance, comparing our *Stenella coeruleoalba* CR sequences to those obtained in the aforementioned databases. Furthermore, a second Neighbour-Joining tree was constructed, comparing the mtDNA sequences from this study, with downloaded sequences (from NCBI nucleotide database) representative of intraspecific variation of other closely related species whenever available (data not shown but available on request). All samples that grouped within monophyletic clades mostly composed of sequences from species other than striped dolphin (on either tree) were removed from the dataset before analysis.

In addition, we carried out another NCBI nucleotide search for the following expression: "Stenella coeruleoalba" AND "control region" AND "D-loop". All sequences that matched the criteria were downloaded and aligned with our own CR dataset. Due to differences in length between the different database sequences, we selected a 336 bp region common to most sequences. The final alignment was representative of most of the worldwide distribution of striped dolphin, and therefore, allowed us to assess whether any haplotype found was representative of the overall variation in this species or not. We did this by calculating a

median-joining network with the software NETWORK (Bandelt et al. 1999), and assessing whether any of the sequences produced in our study created a clade that was particularly divergent relative to the other sequences worldwide.

Spatial Patterns of Genetic Structure and Diversity

To avoid bias from including close kin (Wang, 2018), we calculated pairwise relatedness among all samples. This was done using the Queller and Goodnight Index (r) implemented by GENALEX, using permutation tests with 1 000 iterations, and eliminated one individual from each pair that had an $r \geq 0.5$. A total of 13 individuals were excluded from all subsequent analyses (9 from the Ligurian Sea, 3 from the Adriatic Sea, and 1 from the Ionian Sea). Relatedness within groups was calculated for each population independently. Probability of Identity (PI and PIsib) was calculated using GENALEX (Peakall & Smouse 2006).

Departure from Hardy-Weinberg equilibrium (HWE) was tested for each locus in each population using the Markov chain randomization in GENEPOP (Rousset, 2008) with dememorization number, number of batches and iterations per batch set at 1 000. ARLEQUIN (Excoffier, Laval & Schneider, 2005) was used to assess genotypic disequilibrium among loci with 1 000 permutations. Allelic diversity, observed heterozygosity, and unbiased gene diversity were assessed using GENALEX (Peakall & Smouse, 2006). Allelic Richness was calculated using FSTAT (Goudet, 2001) based on the minimum sample size.

To assess the presence of genetic structure between regional locations, samples were divided into the eight main Mediterranean basins, which have been shown to correlate well with genetic differentiation in other cetacean species (e.g. Gaspari et al., 2015). This included the Levantine, Ionian, Adriatic, Tyrrhenian, Ligurian, Balearic and Alboran Seas, and lastly the Eastern North Atlantic, as represented by samples from Scotland. Differentiation was tested by calculating pairwise Φ_{ST} values between all locations using the software ARLEQUIN, with distance based on pairwise differences. Population genetic summary statistics were also calculated for each location, as described above. We also carried out a Principal Component Analyses on individual genotypes using GENALEX (Peakall & Smouse, 2006). Differentiation between locations was tested by carrying out a one-way NPMANOVA on Euclidean distances between PCA scores for principal components 1 and 2 in the software PAST (Hammer et al., 2001).

We estimated the number of genetic clusters (K) using the Bayesian hierarchical approach implemented in STRUCTURE (Pritchard, Stephens & Donnelly, 2000). We first estimated the most likely number of clusters considering the whole sample set, and then for

each inferred cluster individually, until no more sub-divisions could be detected. We assumed an admixture model with correlated allele frequencies, without specifying sampling locations or putative population origin of samples. The model was run for clusters (K) 1 to 20, using a burn-in period of 150 000 iterations followed by 1 000 000 Markov chain Monte Carlo (MCMC) iterations. Five independent runs were conducted for each value of K to check for convergence. Choice of K was based on comparison between the number of clusters (K) showing the maximum estimated mean log-likelihood of the data (LnP(D)) (Pritchard et al., 2000), and the results from ΔK transformation (Evanno *et al.* 2005), both calculated using STRUCTUREHARVESTER (Earl & vonHoldt, 2012).

We complemented this with the spatially explicit analyses implemented in GENELAND (Guillot, Santos & Estoup, 2008). The model with correlated allele frequency was used, and 4 independent runs consisting of 10 000 000 MCMC steps after 2 000 000 burn-in steps were carried out. Coordinate uncertainty was set to 20 miles, to reflect the species mobility and/or carcass drift in the case of stranded samples.

Temporal patterns of genetic variability

Population genetic summary statistics were calculated for microsatellite genotypes between 1987-2009, using a sliding window of three-years and one-year steps (samples from outside the Mediterranean were not included, because of the known patterns of genetic differentiation between the Atlantic and the Mediterranean; Garcia-Martinez et al., 1999; Bourret et al., 2007; Gaspari et al., 2007; Gkafas et al., 2017). This strategy was adopted for three main reasons: sampling size was uneven between years, so pooling ensured statistical tests and descriptors were based on large enough sample sizes. Striped dolphins are both long lived and have overlapping generations, and therefore, samples from different years are not truly independent. The alternative of considering individual years would not reflect this biological reality, and thus a sliding window of three-years and one-year steps provides the best strategy to minimize unequal sampling throughout the study period.

Genetic diversity statistics including observed/expected heterozigosity, unbiased heterozygosity and F_{IS}, was calculated in GENALEX. Because sample size tends to be higher for recent years, we recalculated genetic diversity statistics using two alternative sample size trimming strategies, and analysed correlation between sample size and F_{IS} using regression analysis (see Supplementary Methods for details). Deviations from Hardy-Weinberg as well as linkage-disequilibrium between loci were calculated in ARLEQUIN. To test for the presence of periodicities in the time series genetic statistics, we applied 3 different time-series

statistical tests: least square spectral analyses for unevenly sampled data (Lomb periodogram); a multitaper spectral analyses with number of tapers set to 3 which retains information on the first and last data point; and a continuous wavelet transformation which simultaneously inspects periodicities at different time scales. All time series tests were carried out using the software PAST v2.17 (Hammer, Harper & Ryan, 2001).

In order to evaluate possible changes in the population social organization, we also analysed patterns of group size and group composition, based on observational data collected from free-ranging dolphins during dedicated summer surveys in the Ligurian Sea. Given that the Ligurian Sea is also the basin that is best represented in our dataset, a comparison between patterns of genetic structure and group composition through time are possible. Patterns of group size from the Ligurian Sea, collected by the Tethys Research Institute during dedicated summer field research campaigns, and stranding data from the Italian peninsula, downloaded from the Italian strandings network database (http://mammiferimarini.unipv.it/) were also analysed for the same time period. The purpose of this analysis was to evaluate whether changes in the genetic patterns would correlate with potential changes in group dynamics. Group size data was divided into number of adults and number of juveniles (newborn, calves and juveniles) per group sighted. Groups were defined as dolphins observed in apparent association, moving in the same direction and often, but not always, engaged in the same activity. Three age classes were defined based on visual assessment of body sizes compared to average adult size: 1. *newborn* and *calves*, below 1/2 of an adult length; constantly in close association with an adult; dorsal fin typically low and rounded; dark, lead-grey coloration with visible foetal creases; immature swimming style with stereotyped surfacing pattern when breathing; calves about 1/2 of an adult; in clear association with an adult, but not as strictly as a *newborn*; light grey coloration, occasionally brownish, usually lighter vertical striping left by foetal creases; 2. *juvenile*, about 2/3 of an adult; usually swimming in association with an adult but sometimes independently; coloration generally slightly lighter than the adult; 3. *adult*, approximately 1.8-2.3 m.

Average number of adults and juveniles in a group was then calculated for a moving average of three years with a one-year step, to investigate any trends of group size and composition in response to the epizootics. Furthermore, changes in the number of pods with and without juveniles as well as the total number of adults and juveniles, was assessed using analyses of covariance (ANCOVA). Changes in the number of juveniles per adults over the years, was assessed through a Spearman correlation test.

Correlation between changes in various time series values was assessed using a cross-

correlation test with varying time lags, as implemented in the software PAST v2.17 (Hammer et al. 2001). Specifically, we tested for cross-correlation between F_{IS} and: number of loci with linkage disequilibria; number of loci with Hardy-Weinberg deviations; the number of adults per group; and the number of juveniles per group. We also tested for cross-correlation between the number of adults and number of juveniles (both per group).

Phylogeographic analyses

Phylogenetic networks of CR haplotypes were inferred using the median-joining method implemented in NETWORK (Bandelt, Forster & Röhl, 1999), and the minimum-spanning method implemented in ARLEQUIN (Excoffier et al., 2005). Haplotypes were classified according to geographic location to assess the presence of spatial structure, and also by year of sampling to assess changes in inference from different time periods.

Historical demography was assessed through calculation of a mismatch distribution between all haplotypes, using the software ARLEQUIN. Timing of mismatch distribution modes was calculated using the formula $T = \tau/2U$ (τ - mismatch mode of interest; U - mutation rate for the whole sequence analysed) as described in (Gaspari *et al.*, 2015).

Furthermore, historical demography was estimated using the Bayesian Skyline method implemented in BEAST (Drummond et al. 2012). The model of nucleotide substitution used in the analyses was determined in TOPALi (Milne et al. 2009), and an uncorrelated relaxed clock was defined with a lognormal prior of mean 0.1 and standard deviation of 0.33. The MCMC chain was run for 10 000 000 iterations, with a sampling frequency of 1 000.

RESULTS

Comparison of CR sequences with other dolphin species

Our GenBank searches retrieved 72 sequences from 21 different dolphin species that are closely related to striped dolphin. From the 131 sequences genotyped in this study for CR, 16 were found to group within clades mostly consisting of other species, with 6 grouping with bottlenose dolphins (genus *Tursiops*) and 10 grouping with common dolphin (genus *Delphinus*). Because both these species occur in the same areas as striped dolphin, they likely represent misidentifications, and were therefore removed from the analyses. Of these, 15 had also been genotyped for microsatellites and were therefore also removed from microsatellite based analyses. Therefore, and also taking into account samples that were removed form the original dataset during our data processing workflow (as detailed in the Methods), all results presented are for a total samples size of 334 for microsatellite data, and 115 for mtDNA.

Information on these samples is available at the end of the supplementary information file (Table S5).

Spatial Patterns of Genetic Structure and Diversity

Population genetic statistics were calculated for the eight main Mediterranean Sea basins included in this study (Table 1). Probability of Identity across microsatellites loci was low in all populations. Four pairs of samples were found to have matching genotypes and therefore, one individual from each pair was excluded, resulting in 364 samples overall. The number of alleles per locus ranged from 6.4 to 14.7, and allelic richness ranged from 5.3 in the Adriatic to 7.6 in Scotland. The highest number of private alleles was found in the Ligurian Sea and in the Ionian Sea. The Balearic and the Adriatic Sea had no private alleles. Values of F_{IS} were generally low, except for Adriatic and Levantine regions, however, most appeared to be significantly higher than 0, with the exception of the Balearic Sea. Significant departure from HWE was observed after Bonferroni correction, but without any clear pattern between loci/geographic region. No loci deviated from HWE at more than 3 geographic regions, and only Ligurian and Adriatic had more than 3 loci which deviated from HWE. Neither Alboran nor Balearic had any loci that deviated from HWE. ARLEQUIN indicated linkage disequilibrium between some loci in different populations possibly due to significant Heterozygosity deficiency (data not shown).

Overall, pairwise F_{ST} values were low but still significant for many comparisons (Table 2). CR showed similar weak differentiation within the Mediterranean, but significantly high Φ_{ST} values between Atlantic and the Mediterranean. Analyses of PCA only found evidence for differentiation between the Mediterranean and the Atlantic, but not within the Mediterranean (Figure S1; Table S3).

The hierarchical population structure analysis implemented in STRUCTURE, collectively suggested that K=2 was the most likely number of clusters, separating the Mediterranean Sea and the eastern north Atlantic. K=2 was the best supported value for the whole dataset, both before and after the ΔK correction (Evanno et al., 2005). For the analyses including only the Mediterranean Sea K=2 also had the best support (Figure S2), however the ancestry plots showed no evidence of geographic structure with all individuals being admixed between the two clusters to some degree (Figure S3). Spatially aware analysis using GENELAND showed the presence of several clusters (Figure S4) however, only the one separating the Atlantic from the Mediterranean appears to match with previously suggested biogeographical barriers in the region.

Phylogeographic analysis

Given the high number of mutational steps obtained in the phylogeographic network, we further integrated our CR sequences with other striped dolphin sequences from the entire species distribution, retrieved from GenBank as detailed in the Methods section. We retrieved 148 striped dolphin CR sequences from GenBank, which included samples from the Pacific Ocean, Bay of Biscay, North Sea, USA Atlantic Coast, Japan, and Mediterranean. This analysis showed that striped dolphin sequences produced in this study are all closely related to sequences found elsewhere in the world (Figure S5), and thus we consider this pattern to reflect the high worldwide genetic diversity of this species (see Discussion for more details).

The phylogenetic network revealed two distinct sections, one composed of several equally frequent haplotypes separated by long mutational steps, and another composed of 3 star-shaped clusters connected by various alternative links (Figure 2). There was no correlation between network clades and geographic location of samples, except for the observation that none of the north east Atlantic haplotypes were found in the star shaped section. Moreover, there were no shared haplotypes between Atlantic and the Mediterranean, though sample size for the Atlantic was low.

The two network construction methods were largely consistent, except for the position of the link between the two distinct sections. In the Minimum-Spanning network it linked the star shaped section to a distinctive haplotype from the Alboran Sea (Figure 2), while in the Median-Joining network it was linked through inferred intermediate haplotypes.

The mismatch distribution was bimodal, and statistical analyses failed to reject both the spatial and the demographic expansion model. However, visual fit of the simulated models with observed data was poor, and highly skewed towards the lowest mode, likely representing the star-shaped section of the phylogeny, characteristic of a demographic expansion (Figure 3).

Temporal calibration of expansion models, suggest a post-glacial expansion for the star-shaped phylogeny section, with an older timeframe for the separation between the two main sections (Table S4). Bayesian skyline reconstruction of historical demography was consistent with a post-glacial demographic expansion (Figure S6), although there is less information from older time periods.

Temporal patterns of genetic variability

The temporal patterns of F_{IS} through our time series show highest values of inbreeding coincident with the two best described epizootics (Figure 4A). Furthermore, a large increase

in F_{IS} is seen for a third period between 1997 and 1999. The estimated value of F_{IS} in 1995 is likely imprecise as a result of low sample size for that year, as indicated by the large error values in the estimate. The observed cyclical changes in these statistics do not appear to result from differences in sample size for each year. Although sample size does change between years, our trimming analyses also showed that uneven sample sizes do not systematically underestimate F_{IS} values (Figure S7), and neither does the relative representation of stranded *vs* biopsy samples (Figure S8). This is further confirmed by the lack of correlation between the number of samples (overall, stranded and biopsies) and the corresponding F_{IS} estimates (Figure S9). Therefore, we kept the full dataset in order to maximize sample size in all statistical tests carried out.

Tests for periodicity in F_{IS} time series all showed evidence for non-random cyclical changes. The least square spectral analyses (Lomb periodogram) revealed a cycle frequency of 9.4 years, with a borderline p-value of 0.052 (Figure 5A). The multitaper spectral analyses revealed a similar cycle of 9.1 years below the significance value of 0.05, while the continuous wavelet transformation (CWT) showed significant results at the range between roughly 5 and 7 years (Figure 5B & 5C). Tests on other genetic statistics were consistent in retrieving cycling periods of between 7-9 years, but were non-significant, apart from the CWT which was significant for all tests (data not shown).

The number of loci that significantly deviate from HWE, as well as the number of pairwise loci in linkage disequilibrium, increases during epizootic events (Figure 4B). The only exception was for the number of LD loci during the years before the first epizootic (1988-1989), however no data prior to that is available. Cross-correlation tests showed significantly positive correlations between the number of loci with LD and HWD, with no time lag (Figures 6A & 6B). There are further significant cross-correlations (both positive and negative) at time lags between 4 and 8 years for both LD and HWD loci, however interpretation of these is confounded by the periodicities identified in all time series.

Group size and composition data for most of the period analysed, shows number of adults in a group decreasing after epizootics relative to the epizootic peaks (Figure 4C). Contrastingly, number of juveniles appears to increase after the epizootic events, slowly diminishing until the next epizootic, with a corresponding increase of the number of adults in the same time frame (approximately 5-6 years; Figure 4C). Although numeric differences between highs and lows are small, this is mostly due to a large number of groups without juveniles. These patterns are confirmed by cross-correlation analyses, which show a positive correlation between number of juveniles and F_{IS} with a two year lag for juveniles (Figure 6D).

In other words, increases in F_{IS} are followed by an increase in juveniles around two years later. As in previous correlations, there are significant correlations at lag times of 7-8 years which likely reflect the periodicities in F_{IS}. For adults, there is also a significant positive cross-correlation with F_{IS}, with a time lag of 6 years for the number of adults (Figure 6C).

Time series plots for the average and total number of juveniles, when considering pods with juveniles only, show a similar trend of juveniles increasing after the epizootics (Figure 7). Interestingly, although over this time period the number of juveniles per year remained overall constant, the number of adults has increased significantly (ANCOVA – Year: $F_{(1,46)} = 22.84$, $P < 0.001$; Figures 7 and S10). This leads to a significant decline in the number of juveniles per adult over the time period analyzed, although this number increases sharply after each epizootic event (Figure S11).

DISCUSSION

Spatial Patterns of Genetic Structure and Diversity

Geographic structure between the Mediterranean basin and the north east Atlantic was identified, consistent with previous studies (Garcia-Martinez et al., 1999; Bourret et al., 2007; Gaspari et al., 2007; Gkafas et al., 2017). However, no strong geographic population structure was found in our fairly comprehensive analysis across the Mediterranean Sea. Although this pattern is apparently in contrast with suggestions from previous studies (Gaspari et al., 2007; Gkafas et al., 2017), several features in our data could potentially account for the apparent discordance. First, nuclear loci show significant F_{ST} levels between many of the Mediterranean Sea basins identified (Table 2). Second, the STRUCTURE result for K=2 showing most individuals having mixed ancestry, can result from various biological scenarios. One involves sampling an admixed population but failing to sample one of the source populations extensively. In this scenario, STRUCTURE is known to identify the number of clusters accurately, but fails to assign the ancestry proportions correctly making most individuals appear admixed (Haasl & Payseur, 2010). Furthermore, the presence of a panmictic population, where some level of genetic heterogeneity in the distribution of genetic variability exists (e.g. isolation-by-distance; Frantz, Cellina, Krier, Schley & Burke, 2009) might lead to a similar pattern. Finally, CR shows patterns of variation consistent with a recent expansion, while also showing haplotypes with a relatively large number of mutations between them. The star-shaped section of the network includes only haplotypes found within the Mediterranean, while the other section of the network includes haplotypes from both the Mediterranean and North Atlantic. This is consistent with a scenario involving past

differentiation between Mediterranean and Atlantic, followed by a recent expansion inside the Mediterranean

If the striped dolphins have developed regional differentiation within the Mediterranean Sea during the Pleistocene glaciations as suggested earlier (Gkafas et al., 2017), but have since experienced a demographic expansion, this could have led to a geographical shuffling of the previously differentiated groups. A similar recent expansion within the Mediterranean Sea was reported for *Tursiops truncatus* (Gaspari et al., 2015) which could have been driven by the same environmental process. However, the relatively deep differentiation between some Mediterranean haplotypes suggests the potential for longer term residence in the area as suggested earlier (Gkafas et al., 2017). Higher resolution genetic data is clearly needed to fully resolve the details regarding historical demographic and population geographic structure of this species in the Mediterranean.

Temporal patterns of genetic variability

Our comprehensive time-series analyses show that patterns of genetic composition in striped dolphins have fluctuated significantly during the 21 year study period. This suggests that patterns of genetic composition inferred from wild samples, can partly reflect demographic patterns that are dynamic in time and not long lasting, potentially confounding inference across geographic locations. For example, in our dataset, higher F_{IS} values for some regions mostly reflect a chronological effect. Many of the samples from the Adriatic Sea were collected in 1997, a period of generally higher F_{IS} values across the Mediterranean. Removal of the 1997 Adriatic samples did not significantly change the time-series plot. Contrastingly, we found no systematic overrepresentation of geographic regions in any of the periods where F_{IS} either peaks or grounds, suggesting that in our dataset, most of the changes occur at a chronological scale.

Similarly, tests for Hardy-Weinberg equilibrium (HWE) and linkage disequilibrium show regular temporal cycles that are consistent in time with changes in other genetic descriptors. Although significant LD and deviations from HWE were found in certain geographic regions, these results may be confounded by the temporal cycles of LD and HWE deviations. This temporal heterogeneity in LD and HWE deviations, could also explain why Bayesian methods that look for clustering patterns that maximize within group HWE consistently failed to give biologically meaningful results, particularly those that were spatially explicit.

Sample sizes were small for some time periods; however, trimming of samples from the overrepresented years did not change inference. We find no evidence that the observed

485 fluctuations would bias inference regarding geographic patterns of population structure
486 calculated at different time points. Nevertheless, in our study it appears that the most
487 significant differences in genetic composition are found along a temporal scale, as opposed to
488 between geographic locations.
489 The cyclical changes in population genetic descriptors through time correlate with the
490 timing of previously described morbillivirus epizootics. Although our data cannot provide
491 definite evidence of a causative relationship, several elements suggest this might be the case.
492 Our time-series analysis show that population F_{IS} levels are low before the epizootics, peak as
493 the epizootic develops, lowering afterwards, and that these F_{IS} fluctuations are significantly
494 different than expected by chance. The sharp increases in F_{IS} are consistent with the two
495 better described epizootic events (1990-1992 and 2006-2008; Van Bressem et al., 2014), and
496 with a third event between 1997 and 1999 for which there is also evidence (though weaker
497 than for the other two epizootics) from serological essays (Van Bressem et al., 2001). The
498 suggested cycle of 3-5 years for morbillivirus epizootics in striped dolphin (Di Guardo &
499 Mazzariol, 2013) would predict another epizootic around 2002 and 2004, but no strong
500 genetic footprint appears evident in our genetic analyses, nor is this strongly documented in
501 the literature. Although there is a slight increase in F_{IS} in 2002, this is much smaller as
502 compared to the changes observed in other better documented epizootics. Instead, visual
503 inspection of our genetic time series suggests a morbillivirus epizootic frequency of roughly
504 every 8 years +/- 2 years, which is consistent with our spectral analyses showing significant
505 support for periodicities between 6 and 9 years. Our results would therefore predict another
506 epizootic sometime in 2013-2015, and there are in fact reports of an increase in striped
507 dolphin strandings infected with morbillivirus in the Mediterranean for that period (Casalone
508 et al., 2014), though the infection appears less severe.
509 The correlation between the episodic changes in genetic composition and the incidence of
510 morbillivirus opens the possibility that such changes might be driven by selective sweeps as
511 opposed to changes in population size. Detecting selective sweeps from unlinked
512 microsatellite loci is extremely challenging, and outside of the scope of this study.
513 Nevertheless, we find this correlation between timing of epizootics and strong fluctuations in
514 a number of population genetic descriptors to be a noteworthy result, and raise the possibility
515 that epizootic survival is not stochastic but could involve a genetic component. The 2006-
516 2008 epizootic was milder in terms of mortality rate relative to 1990-1992 (Di Guardo et al.,
517 2013), and data from the Italian stranding network also shows a progressive reduction in the
518 number of strandings in each of the three outbreaks inferred in this study (Figure S12).

519 Therefore, the Mediterranean striped dolphin could be an interesting model to better
520 understand the real time mechanisms of genetic adaptation of pathogenic infection in future
521 studies.
522
523 **Influence of demographic and other ecological factors**
524 Social data collected for 24 consecutive years in one of the sampled locations, also showed
525 correlation with epizootic events, namely with an increase in the number of juveniles after the
526 epizootics. These data are representative of an area strongly affected by the epizootics (the
527 Ligurian Sea), and suggests increased reproduction and recruitment to be occurring. The
528 succeeding levelling off between the number of adults *vs* juveniles across 5-6 years, is
529 consistent with the species maturation time (Calzada, Aguilar, Grau & Lockyer, 1997),
530 suggesting that as the post-epizootic juveniles mature, density-dependent factors might reduce
531 population recruitment and growth (Figure 7). A study on dusky dolphins, has shown that
532 mating frequency tends to reduce with increasing group size (Orbach, Rosenthal & Würsig,
533 2015), consistent with our observations in group size variation and providing a potential
534 mechanism to account for the inferred density-dependent reduction in recruitment.
535 Simultaneously, reduced density after a mortality event could lead to episodes of
536 immigration (as suggested previously; Gkafas et al., 2017), which would not be easily
537 detected in genetic patterns if migrant individuals and/or F1 hybrids are not sampled, but
538 could originate individuals with shared genetic ancestry across regions (as found in this
539 study). This could suggest that epizootics result from an increase in the density of susceptible
540 individuals, both due to population growth, as juveniles quickly lose their maternal immunity
541 (Van Bressem et al., 2014), and/or immigrants which would have not been previously
542 exposed to the virus.
543 Our long term group size data is also consistent with this interpretation, as the number of
544 adults appears to increase significantly over time, while the number of juveniles does not.
545 Given the long life expectancy of these animals, it is likely that some individuals will remain
546 in the population through the various epizootics. If epizootic survival does indeed have a
547 genetic component (as speculated above), then it would be expected that reduced adult
548 mortality would increase the number of adults relative to juveniles. Although our group
549 composition data was geographically restricted, it does suggest that successive epizootics
550 have not only changed the genetic composition of striped dolphins, but could have also
551 changed its age structure.

552 This system thus appears to be a prime candidate for studies on the mechanisms of
553 morbillivirus resistance in cetaceans, particularly as more samples since 2009 are collected.
554 Ideally, this would involve the study of a large array of immune system genes, as the species
555 undergoes the various epizootics.
556
557 **Concluding remarks**
558 Our study shows that continuous long term genetic data of wild animal populations can
559 reveal genetic changes in response to cyclical environmental pressures (morbillivirus
560 epizootics in this case). Contrastingly, comparison of different geographic regions with
561 different environmental conditions showed very little evidence of genetic differentiation.
562 Furthermore, such time series data allowed a more robust interpretation of the relationship
563 between genetic variation and survival to ecological pressures in the striped dolphin.
564 Although rapid population growth and immigration contribute to effective recovery from
565 epizootics, our results suggest the potential for a genetic mechanism of adaptation to the virus.
566 These adaptive processes would have remained very difficult to infer from samples obtained
567 at individual points in time. Further work would aim at understanding whether this potential
568 adaptation results from constant selective pressures or a series of selective sweeps.
569 This study also carries important conservation and animal welfare implications for the
570 Mediterranean biodiversity hotspot, as striped dolphin could represent a potential
571 morbillivirus reservoir in the region. Morbillivirus infection has been in fact, increasingly
572 observed in other marine mammals such as bottlenose dolphins (Di Guardo et al., 2013), fin
573 whales (Mazzariol et al., 2012), and the critically endangered monk seal (van de Bildt et al.,
574 2000), which further emphasize the need to carry out more detailed studies on this biological
575 system.
576
577 **ACKNOWLEDGEMENTS**
578 We want to thank the Prince Albert II of Monaco Foundation for providing most of the
579 funding for this study; we are also grateful to the following institutions for funding
580 contribution: The Society for Marine Mammalogy through the Emily B. Shane Award, the
581 University of Durham, and the Tethys Research Institute. We would also like to thank
582 numerous people who helped collecting samples, and shared tissue samples: Tethys Research
583 Institute (Italy); Cristina Fossi (Italy), Centro Studi Cetacei Italy, M. Domingo (Spain),
584 Alexandros Frantzis, (Greece), Bob Reid (Scotland), Aviad Schenin (Israel). We thank

585 Claudio Ciofi and Elisa Banchi for laboratory support. We also want to acknowledge
586 suggestions made by two anonymous reviewers, which greatly improved the manuscript.
587
588 **REFERENCES**
589
590 Aguilar, A. & Borrell, A. (2005). DDT and PCB reduction in the western Mediterranean from
591 1987 to 2002, as shown by levels in striped dolphins (*Stenella coeruleoalba*). *Marine*
592 *Environmental Research*, 59, 391-404. DOI: 10.1016/j.marenvres.2004.06.004
593 Bandelt, H.-J., Forster, P. & Röhl, A. (1999). Median-joining networks for inferring
594 intraspecific phylogenies. *Molecular Biology and Evolution*, 16, 37-48. DOI:
595 10.1093/oxfordjournals.molbev.a026036
596 Barrett, T., Visser, I. K. G., Mamaev, L., Goatley, L., van Bressem, M.-F. & Osterhaus, A. D.
597 M. E. (1993). Dolphin and porpoise Morbilliviruses are genetically distinct from
598 phocine distemper virus. *Virology*, 193, 1010–1012. DOI: 10.1006/VIRO.1993.1217
599 Bourret, V., Macé, M. & Crouau-Roy, B. (2007). Genetic variation and population structure
600 of western Mediterranean and northern Atlantic *Stenella coeruleoalba* populations
601 inferred from microsatellite data. *Journal of the Marine Biological Association of the*
602 *UK*, 87, 265–269. DOI: 10.1017/S0025315407054859
603 Bourret, V., Macé, M., Bonhomme, M. & Crouau-Roy, B. (2008). Microsatellites in
604 cetaceans: an overview. *The Open Marine Biology Journal*, 2, 38-42.
605 Calzada, N., Aguilar, A., Grau, E. & Lockyer, C. (1997). Patterns of growth and physical
606 maturity in the western Mediterranean striped dolphin, *Stenella coeruleoalba*
607 (Cetacea: Odontoceti). *Canadian Journal of Zoology*, 75, 632-637. DOI: 10.1139/z97-
608 078
609 Casalone, C., Mazzariol, S., Pautasso, A., Di Guardo, G., Di Nocera, F., Lucifora, G., Ligios,
610 C., Franco, A., Fichi, G., Cocumelli, C., Cersini, A., Guercio, A., Puleio, R., Goria,
611 M., Podestà, M., Marsili, L., Pavan, G., Pintore, A., De Carlo, E., Eleni, C. &
612 Caracappa, S. (2014). Cetacean strandings in Italy: an unusual mortality event along
613 the Tyrrhenian Sea coast in 2013. *Diseases of Aquatic Organisms*, 109, 81-86. DOI:
614 10.3354/dao02726
615 Cebrian, D. (1995). The striped dolphin *Stenella coeruleoalba* epizootic in Greece, 1991–
616 1992. *Biological Conservation*, 74, 143-145. DOI: 10.1016/0006-3207(95)00024-x
617 Clutton-Brock, T. H. & Pemberton, J. M. (2004). *Soay sheep: dynamics and selection in an*
618 *island population*. Cambridge University Press: Cambridge, UK.

619 Di Guardo, G. & Mazzariol, S. (2013). Dolphin Morbillivirus: a lethal but valuable infection
620 model. *Emerging Microbes & Infections*, 2, e74. DOI: 10.1038/emi.2013.74
621 Di Guardo, G., Di Francesco, C. E., Eleni, C., Cocumelli, C., Scholl, F., Casalone, C., Peletto,
622 S., Mignone, W., Tittarelli, C., Di Nocera, F., Leonardi, L., Fernández, A., Marcer, F.
623 & Mazzariol, S. (2013). Morbillivirus infection in cetaceans stranded along the Italian
624 coastline: Pathological, immunohistochemical and biomolecular findings. *Research in*
625 *Veterinary Science*, 94, 132-137. DOI: 10.1016/j.rvsc.2012.07.030
626 Drummond, A. J., Suchard, M. A., Xie, D. & Rambaut, A. (2012). Bayesian phylogenetics
627 with BEAUti and the BEAST 1.7. *Molecular Biology and Evolution*, **29**: 1969-1973.
628 DOI: 10.1093/molbev/mss075
629 Earl, D. A. & vonHoldt, B. M. (2012). STRUCTURE HARVESTER: a website and program
630 for visualizing STRUCTURE output and implementing the Evanno method.
631 *Conservation Genetic Resources*, **4:** 359-361. DOI: 10.1007/s12686-011-9548-7
632 Excoffier, L., Laval, G. & Schneider, S. (2005). Arlequin ver. 3.0: An integrated software
633 package for population genetics data analysis. *Evolutionary Bioinformatics Online*, 1,
634 47-50.
635 Evanno G, Regnaut S, Goudet J (2005). Detecting the number of clusters of individuals using
636 the software STRUCTURE: a simulation study. *Mol Ecol* **14**: 2611-2620. DOI:
637 10.1111/j.1365-294X.2005.02553.x
638 Frantz, A. C., Cellina, S., Krier, A., Schley, L. & Burke, T. (2009). Using spatial Bayesian
639 methods to determine the genetic structure of a continuously distributed population:
640 clusters or isolation by distance? *Journal of Applied Ecology*, 46,493-505. DOI:
641 10.1111/j.1365-2664.2008.01606.x
642 Garcia-Martinez, J., Moya, A., Raga, J. A. & Latorre, A. (1999). Genetic differentiation in the
643 striped dolphin *Stenella coeruleoalba* from European waters according to
644 mitochondrial DNA (mtDNA) restriction analysis. *Molecular Ecology*, 8, 1069-1073.
645 DOI: 10.1046/j.1365-294x.1999.00672.x
646 Gaspari, S., Azzelino, A., Airoldi, S. & Hoelzel, A. R. (2007). Social kin associations and
647 genetic structuring of striped dolphin populations (*Stenella coeruleoalba*) in the
648 Mediterranean Sea. *Molecular Ecology*, 16, 2922-2933. DOI: 10.1111/j.1365-
649 294X.2007.03295.x
650 Gaspari, S., Scheinin, A., Holcer, D., Fortuna, C., Natali, C., Genov, T., Frantzis, A.,
651 Chelazzi, G. & Moura, A. E. (2015). Drivers of population structure of the bottlenose

652 dolphin (*Tursiops truncatus*) in the Eastern Mediterranean Sea. *Evolutionary Biology*,
653 42, 177-190. DOI: 10.1007/s11692-015-9309-8
654 Gkafas, G., Exadactylos, A., Rogan, E., Raga, J., Reid, R. & Hoelzel, A. R. (2017).
655 Biogeography and temporal progression during the evolution of striped dolphin
656 population structure in European waters. *Journal of Biogeography*, 44, 2681–2691.
657 DOI: 10.1111/jbi.13079
658 Goudet, J. (2001). FSTAT, a program to estimate and test gene diversities and fixation indices
659 (version 2.9.3). *Available from http://www.unil.ch/izea/softwares/fstat.html.*
660 Guillot, G., Santos, F. & Estoup, A. (2008). Analysing georeferenced population genetics data
661 with Geneland: a new algorithm to deal with null alleles and a friendly graphical user
662 interface. *Bioinformatics*, 24, 1406-1407. DOI: 10.1093/bioinformatics/btn136
663 Haasl, R. J. & Payseur, B. A. (2010). Multi-locus inference of population structure: a
664 comparison between single nucleotide polymorphisms and microsatellites. *Heredity*,
665 106, 158-171. DOI: 10.1038/hdy.2010.21
666 Hammer, Ø., Harper, D. A. T., & Ryan, P. D. (2001). PAST: paleontological statistics
667 software package for education and data analysis. *Palaeontologia Electronica*, 4, art.
668 4.
669 Lipscomb, T. P., Kennedy, S., Moffett, D., Krafft, A., Klaunberg, B. A., Lichy, J. H., Regan,
670 G. T., Worthy, G. A. J. & Taubenberger, J. K. (1996). Morbilliviral epizootic in
671 bottlenose dolphins of the Gulf of Mexico. *Journal of Veterinary Diagnostic*
672 *Investigation*, 8, 283–290. DOI: 10.1177/104063879600800302
673 Lovatt, F. M. & Hoelzel, A. R. (2013). Impact on reindeer (*Rangifer tarandus*) genetic
674 diversity from two parallel population bottlenecks founded from a common source.
675 *Evolutionary Biology*, 41, 240-250. DOI: 10.1007/s11692-013-9263-2
676 Mazzariol, S., Marcer, F., Mignone, W., Serracca, L., Goria, M., Marsili, L., Di Guardo, G. &
677 Casalone, C. (2012). Dolphin Morbillivirus and *Toxoplasma gondii* coinfection in a
678 Mediterranean fin whale (*Balaenoptera physalus*). *BMC Veterinary Research*, 8, 20.
679 DOI: 10.1186/1746-6148-8-20
680 Milne, I., Lindner, D., Bayer, M., Husmeier, D., McGuire, G., Marshall, D. F., Wright, F.
681 (2009). TOPALi v2: a rich graphical interface for evolutionary analyses of multiple
682 alignments on HPC clusters and multi-core desktops. *Bioinformatics*, **25**: 126-127.
683 DOI: 10.1093/bioinformatics/btn575
684 Moura, A. E., Natoli, A., Rogan, E. & Hoelzel, A. R. (2013). Atypical panmixia in a
685 European dolphin species (*Delphinus delphis*): implications for the evolution of

686 diversity across oceanic boundaries. *Journal of Evolutionary Biology*, 26, 63-75. DOI:
687 10.1111/jeb.12032
688 Orbach, D. N., Rosenthal, G. G. & Würsig, B. (2015). Copulation rate declines with mating
689 group size in dusky dolphins (*Lagenorhynchus obscurus*). *Canadian Journal of*
690 *Zoology*, 93, 503-507. DOI: 10.1139/cjz-2015-0081
691 Peakall, R. O. D. & Smouse, P. E. (2006). Genalex 6: genetic analysis in Excel. Population
692 genetic software for teaching and research. *Molecular Ecology Notes*, 6, 288-295.
693 DOI: 10.1111/j.1471-8286.2005.01155.x
694 Pilot, M., Dąbrowski, M. J., Jancewicz, E., Schtickzelle, N. & Gliwicz, J. (2010). Temporally
695 stable genetic variability and dynamic kinship structure in a fluctuating population of
696 the root vole *Microtus oeconomus*. *Molecular Ecology*, 19, 2800-2812. DOI:
697 10.1111/j.1365-294X.2010.04692.x
698 Pritchard, J. K., Stephens, M. & Donnelly, P. (2000). Inference of population structure using
699 multilocus genotype data. *Genetics*, 155, 945-959.
700 Rousset, F. (2008). Genepop'007: a complete re-implementation of the genepop software for
701 Windows and Linux. *Molecular Ecology Resources*, 8, 103-106. DOI: 10.1111/j.1471-
702 8286.2007.01931.x
703 Taubenberger, J. K., Tsai, M. M., Atkin, T. J., Fanning, T. G., Krafft, A. E., Moeller, R. B.,
704 Kodsi, S. E., Mense, M.G. & Lipscomb, T. P. (2000). Molecular genetic evidence of a
705 novel Morbillivirus in a long-finned pilot whale (*Globicephalus melas*). *Emerging*
706 *Infectious Diseases*, 6, 42–45. DOI: 10.3201/eid0601.000107
707 Teacher, A. G. F. & Griffiths, D. J. (2011). HapStar: automated haplotype network layout and
708 visualization. *Molecular Ecology Resources*, 11, 151-153. DOI: 10.1111/j.1755-
709 0998.2010.02890.x
710 Turner, A. K., Beldomenico, P. M., Bown, K., Burthe, S. J., Jackson, J. A., Lambin, X. &
711 Begon, M. (2014). Host–parasite biology in the real world: the field voles of Kielder.
712 *Parasitology*, 141, 997-1017. DOI: 10.1017/s0031182014000171
713 Valsecchi, E., Amos, W., Raga, J. A., Podesta, M. & Sherwin, W. (2004). The effects of
714 inbreeding on mortality during a morbillivirus outbreak in the Mediterranean striped
715 dolphin (*Stenella coeruleoalba*). *Animal Conservation*, 7, 139-146. DOI:
716 10.1017/S1367943004001325
717 Van Bressem, M.-F., Waerebeek, K. Van, Jepson, P. D., Raga, J. A., Duignan, P. J., Nielsen,
718 O., Di Beneditto, A. P., Siciliano, S., Ramos, R., Kant, W., Peddemors, V., Kinoshita,
719 R., Ross, P. S., López-Fernandez, A., Evans, K., Crespo, E., Barrett, T. (2001). An

720 insight into the epidemiology of dolphin morbillivirus worldwide. *Veterinary*
721 *Microbiology*, 81, 287–304. DOI: 10.1016/S0378-1135(01)00368-6
722 Van Bressem, M.-F., Duignan, P., Banyard, A., Barbieri, M., Colegrove, K., De Guise, Di
723 Guardo, G., Dobson, A., Domingo, M., Fauquier, D., Fernandez, A., Goldstein, T.,
724 Grenfell, B., Groch, K., Gulland, F., Jensen, B., Jepson, P., Hall, A., Kuiken, T.,
725 Mazzariol, S., Morris, S., Nielsen, O., Raga, J., Rowles, T., Saliki, J., Sierra, E.,
726 Stephens, N., Stone, B., Tomo, I., Wang, J., Waltzek, T. & Wellehan, J. (2014).
727 Cetacean morbillivirus: current knowledge and future directions. *Viruses*, 6, 5145-
728 5181. DOI: 10.3390/v6125145
729 van de Bildt, M. W., Martina, B. E., Vedder, E. J., Androukaki, E., Kotomatas, S.,
730 Komnenou, A., Sidi, B. A., Jiddou, A. B., Barham, M. E., Niesters, H. G. &
731 Osterhaus, A. D. (2000). Identification of morbilliviruses of probable cetacean origin
732 in carcases of Mediterranean monk seals (*Monachus monachus*). *Veterinary Record*,
733 146, 691-694. DOI: 10.1136/vr.146.24.691
734 Van Oosterhout, C., Hutchinson, W. F., Wills, D. P. M. & Shipley, P. (2004). MICRO-
735 CHECKER: software for identifying and correcting genotyping errors in microsatellite
736 data. *Molecular Ecology Notes*, 4, 535–538. DOI: 10.1111/j.1471-8286.2004.00684.x
737 Wang, J. (2018). Effects of sampling close relatives on some elementary population genetics
738 analyses. *Molecular Ecology Resources*, 18, 41–54. DOI: 10.1111/1755-0998.12708

FIGURE LEGENDS

Figure 1 Geographic location of samples used in this study. Red dots denote individual sample location. Blue circles represent provenance of samples that were either stranded or for which there was no information on precise sampling location, and size is proportional to the number of samples.

Figure 2 Minimum spanning network for all CR sequences. Size of the circles is proportional to the number of samples found with the corresponding haplotype. Number of mutational steps represented by vertical bars. Link length not necessarily to scale. Colours represent geographic origin of the samples, with the sizes of circle fraction proportional to number of samples from each region. Network was produced in the software ARLEQUIN, and graphical layout produced with HAPSTAR (Teacher & Griffiths, 2011)

Figure 3 Mismatch distribution for all CR haplotypes. Columns represent the observed distribution. Solid line represents the expected distribution under a demographic expansion model, while dashed line represents the expected distribution under a spatial expansion model

Figure 4 Time-series plot of population genetic statistics for Mediterranean striped dolphin (*S. coeruloealba*). Grey vertical areas represent the years for which morbillivirus epizootics are well described, with are with grey dots representing a less described epizootic. A: F_{IS} - inbreeding coefficient; Solid horizontal line represents $F_{IS} = 0$. B: # HWD loci - number of loci with significant deviations from Hardy-Weinberg equilibrium; # LD loci - number of loci pairs with significant tests for linkage disequilibrium. C: time-series plot of F_{IS} against average number of adults and juveniles in a group, from direct observation data. Each data point represents samples pooled from three different years, with the date representing the central year (e.g. 1988 includes samples from 1987, 1988 and 1989). See text for further details on the calculations

Figure 5 Results from statistical tests of periodicities in the F_{IS} time series data. From left to right, plots are presented for a least square spectral analyses (power axis represents the square amplitude of sinusoids at the corresponding frequency), multitaper spectral analyses with 3 tapers (F axis represents the value of the test statistic for significance at the corresponding periodicity), and a continuous wavelet transformation (i axis reflects years along the time

series, and colour scale reflects power of correlation between wavelet frequency at the corresponding time series). Dashed lines represent the 0.05 significance threshold in all plots.

Figure 6 Results of cross-correlation plots between time-series data, for different time lag values. Comparisons are shown between A: F_{IS} and number of loci in Hardy-Weinberg disequilibrium (HWD); B: F_{IS} and number of loci in linkage disequilibrium (LD); C: F_{IS} and number of adults per group; D: F_{IS} and number of juveniles per group. Dashed lines represent the p-values for each time lag class.

Figure 7 Time-series plots for the mean number of individuals per pods with and without juveniles, as well as the average number of juveniles per pod. Each value represents a yearly estimate. Grey vertical areas represent the years for which morbillivirus epizootics are well described, and area with grey dots representing a less described epizootic (see main text).

LIST OF SUPPORTING INFORMATION

Table S1 Number of stranded and biopsy samples used per geographic region, N - total number of samples analysed; s – stranded samples; fr – free ranging samples.

Table S2 – Annealing temperatures for the multiplex microsatellite PCRs carried out in this study.

Table S3 Results of pairwise NPMANOVA of PCA scores, between all basins analysed in this study. P-values are represented above the diagonal, while significance after Bonferroni correction (**) is presented below the diagonal. PCA plot can be found in Figure S1.

Table S4 Time calibration for both modal peaks of the mismatch distribution, and the τ from the simulated expansion model, following the method used in (Gaspari et al., 2015). μ - mutation rate in substitutions/site/million years; U - mutation rate in substitution/locus/million years.

Table S5 Details on final sample set used in this study. All samples were genotyped for microsatellites. CR haplotype numbers reflect the designation shown in Figure S5. Samples

obtained from GenBank included at the end of table, with no information on year, source and sex shown.

Figure S1 PCA plot based on individual microsatellite genotypes presented in this study. Polygons represent convex hulls around samples from the 7 main Mediterranean basins and Scotland.

Figure S2 These plots show support for the different values of K tested with the STRUCTURE software. A – represents the mean likelihood and standard deviation for all 20 runs based on the whole dataset. B – represents the mean likelihood and standard deviation for all 20 runs based only on the Mediterranean samples. The plots were produced using STRUCTUREHARVESTER (Earl & vonHoldt, 2012).

Figure S3 Individual ancestry plot for K values 2-4, obtained from the analyses including all samples. Plot produced by permutation cluster assignment between individual runs using CLUMPP (Jakobsson & Rosenberg, 2007), with graphical output produced using DISTRUCT (Rosenberg, 2003).

Figure S4 Geographic distribution of clusters, inferred by the spatially explicit model applied in GENELAND (Guillot et al., 2008).

Figure S5 Median-Joining network of striped dolphin CR sequences, representative of most of the species worldwide distribution. Light green - samples used in this study; dark green - sequences retrieved from GenBank; small red circles – haplotypes inferred to exist but not sampled. Note that sequences produced in this study are mostly from the Mediterranean (with some from Scotland), while sequences from GenBank were obtained worldwide. All of the sequences produced in this study are well within the overall variation found in striped dolphins worldwide. The worldwide mtDNA control region network produced here is consistent with the expectations for a population with large stable N_e for long periods of time.

Figure S6 Bayesian skyline reconstruction of historical demography based on Mediterranean striped dolphin CR data, using the BEAST software (Drummond et al., 2012). Estimated mutation rate was 0.16 mutations/site/million years.

Figure S7 Comparison plots between the different sampling schemes used to assess bias from uneven sample size between years, for key genetic diversity measures. Details of trimming strategies are provided at the top of this supplementary document. N – sample size; F_{IS} – inbreeding coefficient; H_O – observed heterozygosity; H_E – expected heterozygosity. Although the time series plots changes slightly between datasets, our data interpretation did not change, with the correlation between increased F_{IS} and the peak of epizootics still remaining.

Figure S8 Number of biopsy and stranded samples for each year of the time-series analysed in this study.

Figure S9 Plot relating sample number for each of the time periods in our temporal analyses (total and biopsies represented in the lower x-axis, stranded represented in the top x-axis) and corresponding F_{IS} values. The plot shows lack of correlation between F_{IS} values and the number of either stranded or biopsy samples, suggesting there is no systematic bias resulting from numbers of stranded or biopsy samples.

Figure S10 Time-series plots for the total number of individuals observed per year, in pods with and without juveniles, as well as the total number of juveniles observed per year. Grey bars represent the years of the three morbillivirus epizootics which are consistent with inference from the genetic data (see main text).

Figure S11 Time series plot for the average number of juveniles per adults, in pods observed in a given year. Grey bars represent the years of the three morbillivirus epizootics which are consistent with inference from the genetic data (see main text).

Figure S12 Time-series plot for the number of strandings recorded during the data period for which we have genetic information. Left - Italian coast; Right- Ligurian sea (http://mammiferimarini.unipv.it/spiaggiamenti.php).

TABLES

Table 1. Population genetic summary statistics, calculated for each region (see Figure 1), using both microsatellites and CR. N - number of samples; AR - allelic richness; NA - average number of alleles across loci; mean PA - average number of private alleles across loci; He - expected heterozygosity; Ho - observed heterozygosity; r - average pairwise relatedness index; F_{IS} - inbreeding coefficient; PI – probability of identity; PS – number of polymorphic sites; NH - number of haplotypes; π - average pairwise nucleotide differences; D - Tajima's D; Fs - Fu's F. *-significant at the 0.05 threshold, ** significant at the 0.01 threshold.

Microsatellites

Sea Region	N	AR	NA	Mean PA	He	Ho	r	F_{IS}	F_{IS} p-value	PI (unbiased)	PI(sib)
Alboran	21	5.48	8.1	0.067	0.720	0.698	-0.050	0.058	0.038	5.2×10^{-16}	1.8×10^{-6}
Balearic	14	5.30	6.7	0.067	0.699	0.733	-0.080	-0.013	0.674	3.8×10^{-15}	2.8×10^{-6}
Ligurian	190	5.71	14.5	1.667	0.749	0.679	-0.005	0.073	0.000	2.2×10^{-17}	8.9×10^{-7}
Tyrrhenian	34	5.87	10.7	0.533	0.744	0.685	-0.031	0.095	0.000	2.3×10^{-17}	9.5×10^{-7}
Adriatic	16	5.27	6.9	0.000	0.699	0.573	-0.069	0.219	0.000	3.5×10^{-15}	2.8×10^{-6}
Ionian	39	5.13	9.2	0.400	0.691	0.645	-0.027	0.084	0.000	5.5×10^{-15}	3.4×10^{-6}
Levantine	8	5.83	6.1	0.133	0.718	0.540	-0.143	0.294	0.000	1.2×10^{-16}	1.9×10^{-6}
Scotland	12	6.98	8.9	0.467	0.800	0.761	-0.091	0.100	0.000	9.0×10^{-20}	2.5×10^{-7}

CR

Sea Region	N	PS	NH	π	H	D	Fs
Alboran	19	38	19	0.011 (0.002)	1.000 (0.017)	-0.261	-11.21**
Balearic	12	37	12	0.013 (0.002)	1.000 (0.034)	-0.160	-4.37*
Ligurian	45	64	45	0.012 (0.001)	1.000 (0.005)	-0.701	-24.52**
Tyrrhenian	12	39	12	0.016 (0.002)	1.000 (0.034)	-0.479	-4.44*
Adriatic	1	0	1	0.000 (0.000)	-	-	-
Ionian	15	20	13	0.008 (0.003)	0.981 (0.031)	0.527	-4.87*
Levantine	4	4	4	0.002 (0.001)	1.000 (0.177)	-0.065	-1.74*
Scotland	7	27	7	0.011 (0.001)	1.000 (0.037)	0.503	-1.29

883

884 **Table 2.** Pairwise Φ_{ST} values between main geographic regions within the Mediterranean Sea,
885 and in comparison to Scotland. Microsatellite values represented below the diagonal, while
886 CR values are above the diagonal. Significance is represented by * - significant at 0.05; ** -
887 significant at 0.001.

888

	Alboran	Balearic	Ligurian	Tyrrhenian	Adriatic	Ionian	Levantine	Scotland
Alboran	-		-0.001	-0.044	-0.570	-0.019	0.047	0.330**
Balearic	0.011	-		-0.037	-0.458	0.088*	0.130	0.273**
Ligurian	0.007*	0.013**	-	-0.033	-0.544	0.008	0.048	0.314**
Tyrrhenian	0.008	0.012*	0.004*	-	-0.594	-0.008	0.066	0.276**
Adriatic	0.015	0.029**	0.008*	0.010	-	-0.531	-0.733	0.333
Ionian	0.007	0.018**	0.008**	0.010**	0.002	-	0.061	0.438**
Levantine	0.012	0.017	0.013*	0.011	0.027	0.025*	-	0.557**
Scotland	0.075**	0.058**	0.076**	0.062**	0.099**	0.093**	0.051**	-

889

890

Figure 1

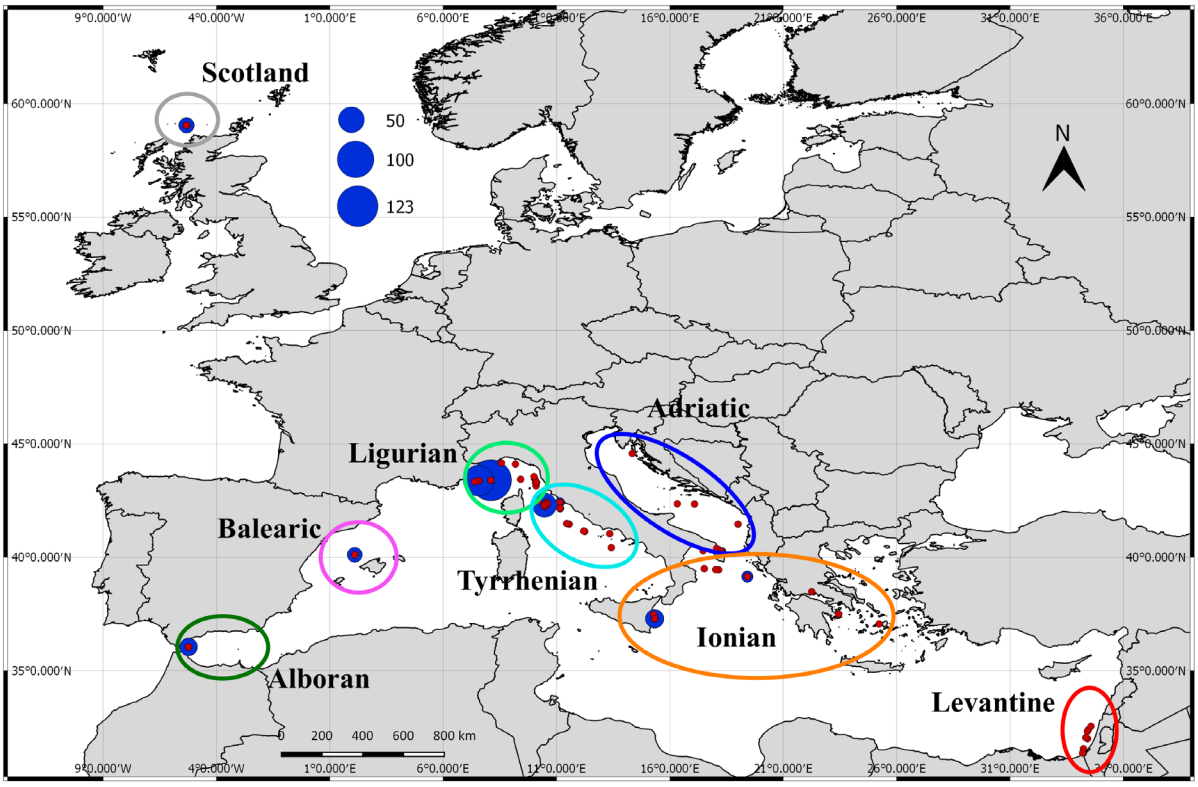

Figure 2

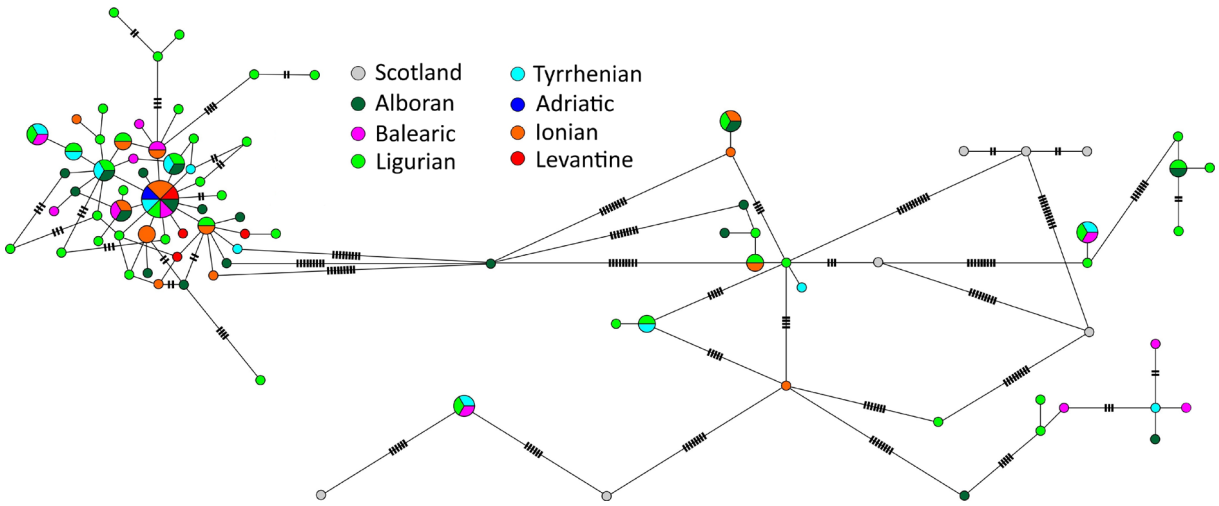

900 **Figure 3**

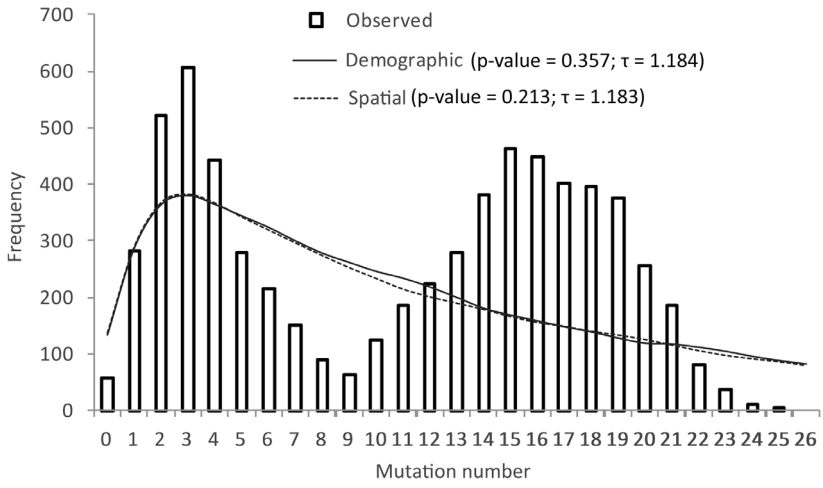

901

902 **Figure 4**

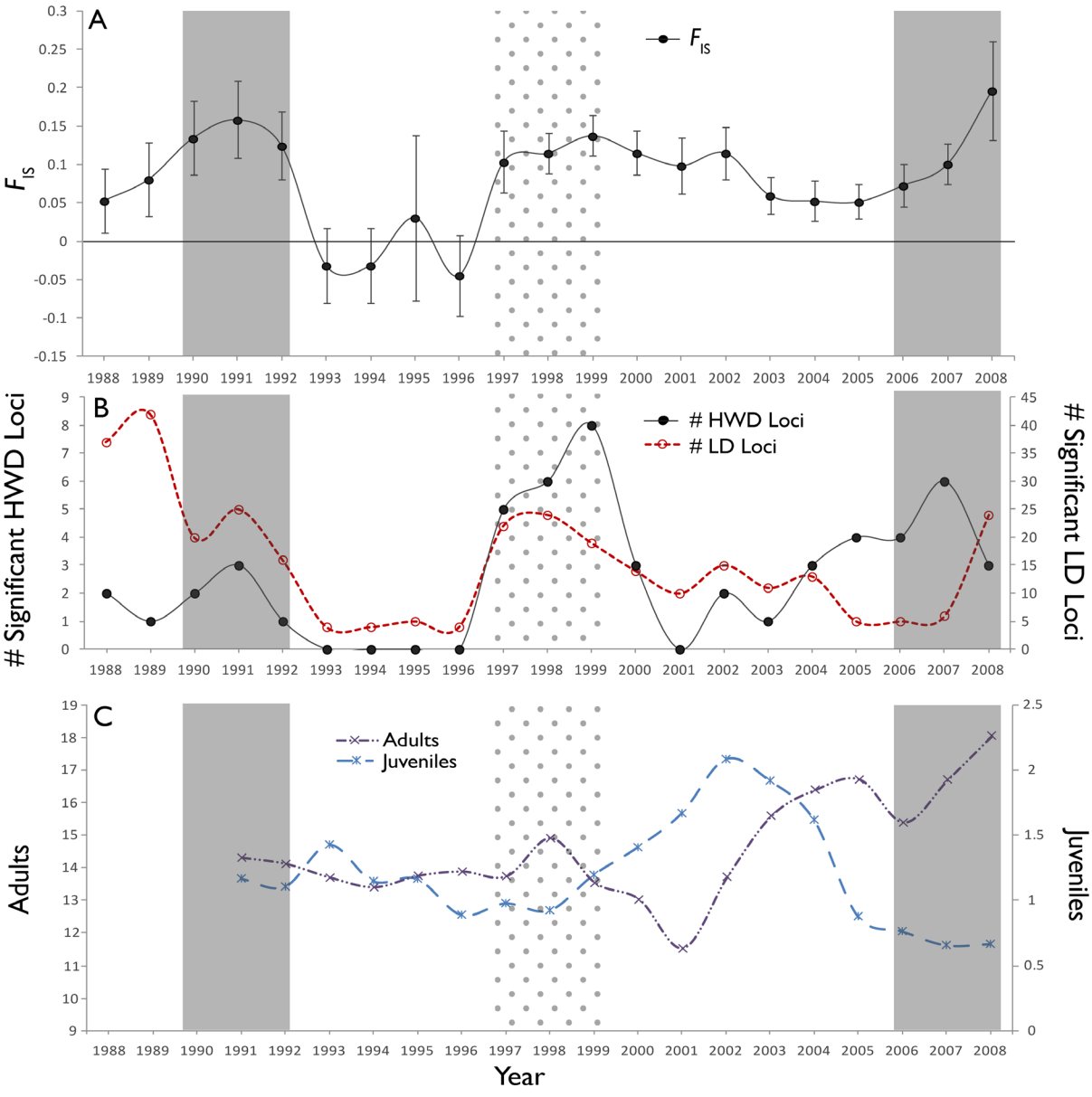

903

Figure 5

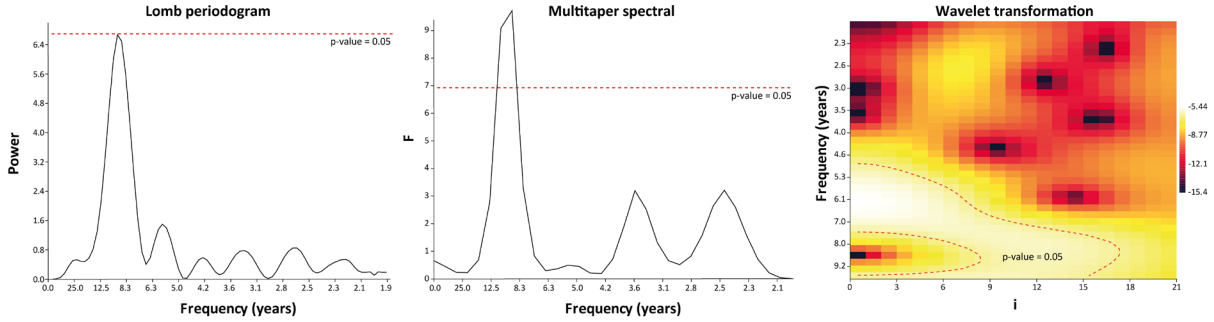

Figure 6

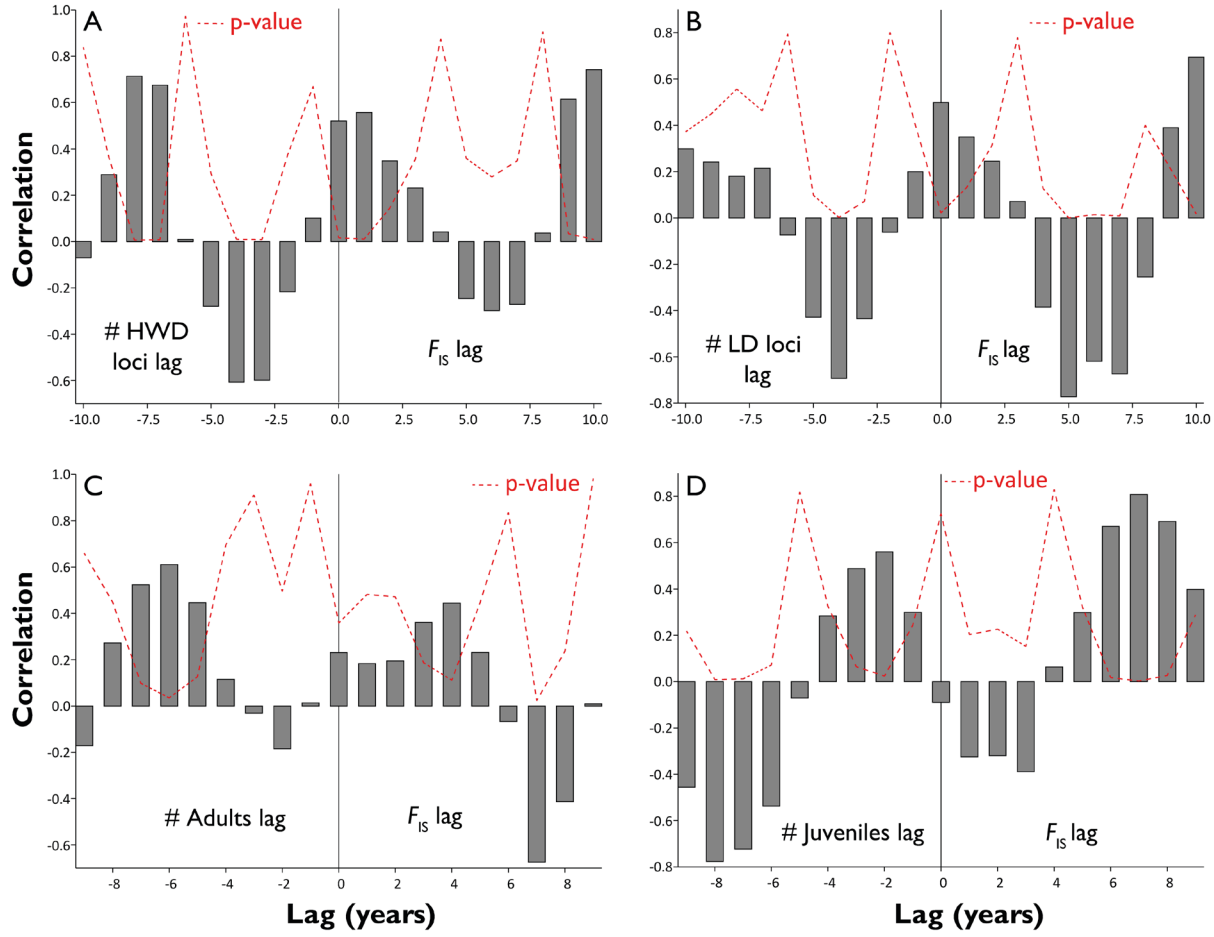

911 **Figure 7**

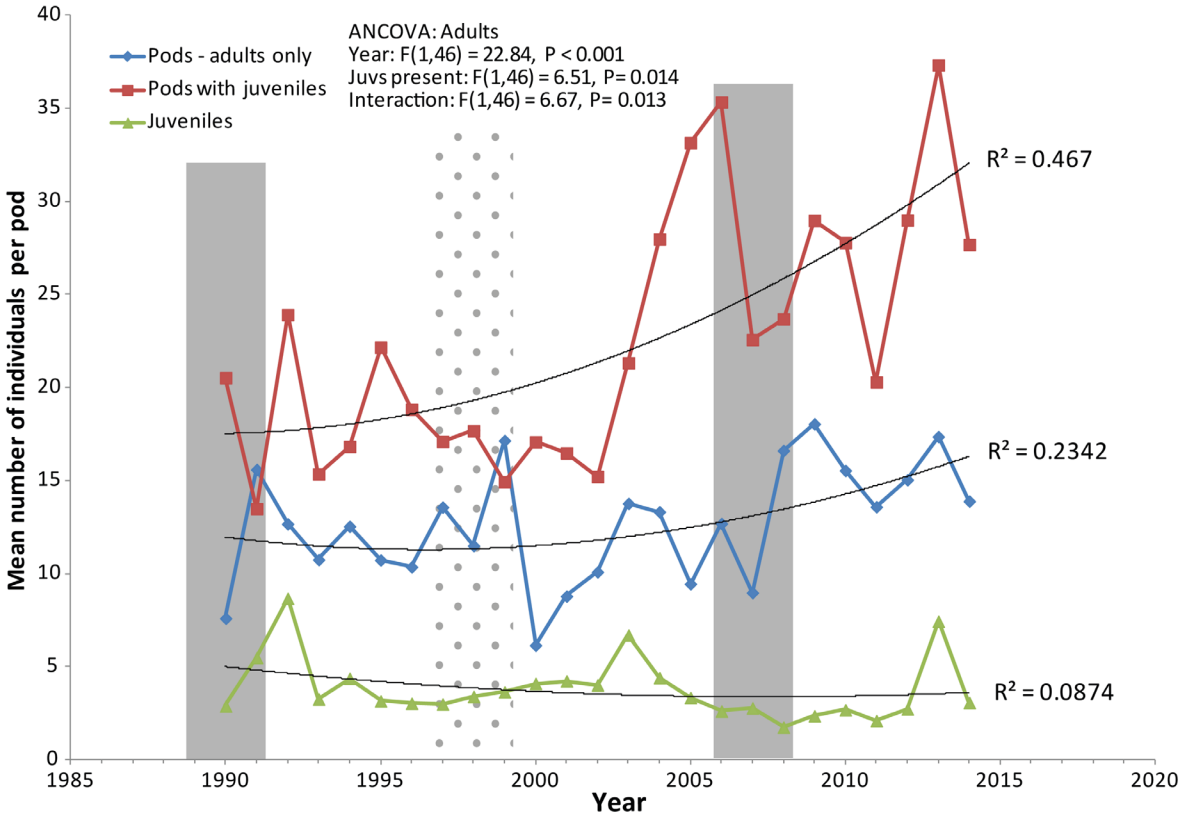

912

913